Supporting Information for

MWIR-LWIR Dual-Band Imaging System with Hybrid Refractive-Diffractive-Metasurface optics for Spatially Separated Focal Planes

Zhiang Qian (钱志昂)[1], Bingxia Wang (王炳霞)[1*], Bowei Xia (夏博威)[2], Zhihao He (贺志豪)[1], Xinyi Lei (雷欣怡)[1], Jianbao Xu(徐健宝)[1], Jierong Gu (顾杰荣)[3], Xiang Shen (沈祥)[1], and Shuming Wang (王漱明)[4]

[1]Laboratory of Infrared Materials and Devices, Research Institute of Advanced Technologies, Key Laboratory of Photoelectric Detection Materials and Devices of Zhejiang Province, Ningbo University, China

[2]Laboratory of Intelligent Collaborative Computing, University of Electronic Science and Technology of China, Chengdu, 611731, China

[3]Ningbo Institute of Oceanography, Ningbo 315832, China

[4] National Laboratory of Solid-State Microstructures, School of Physics, Nanjing University, Nanjing 210093, China

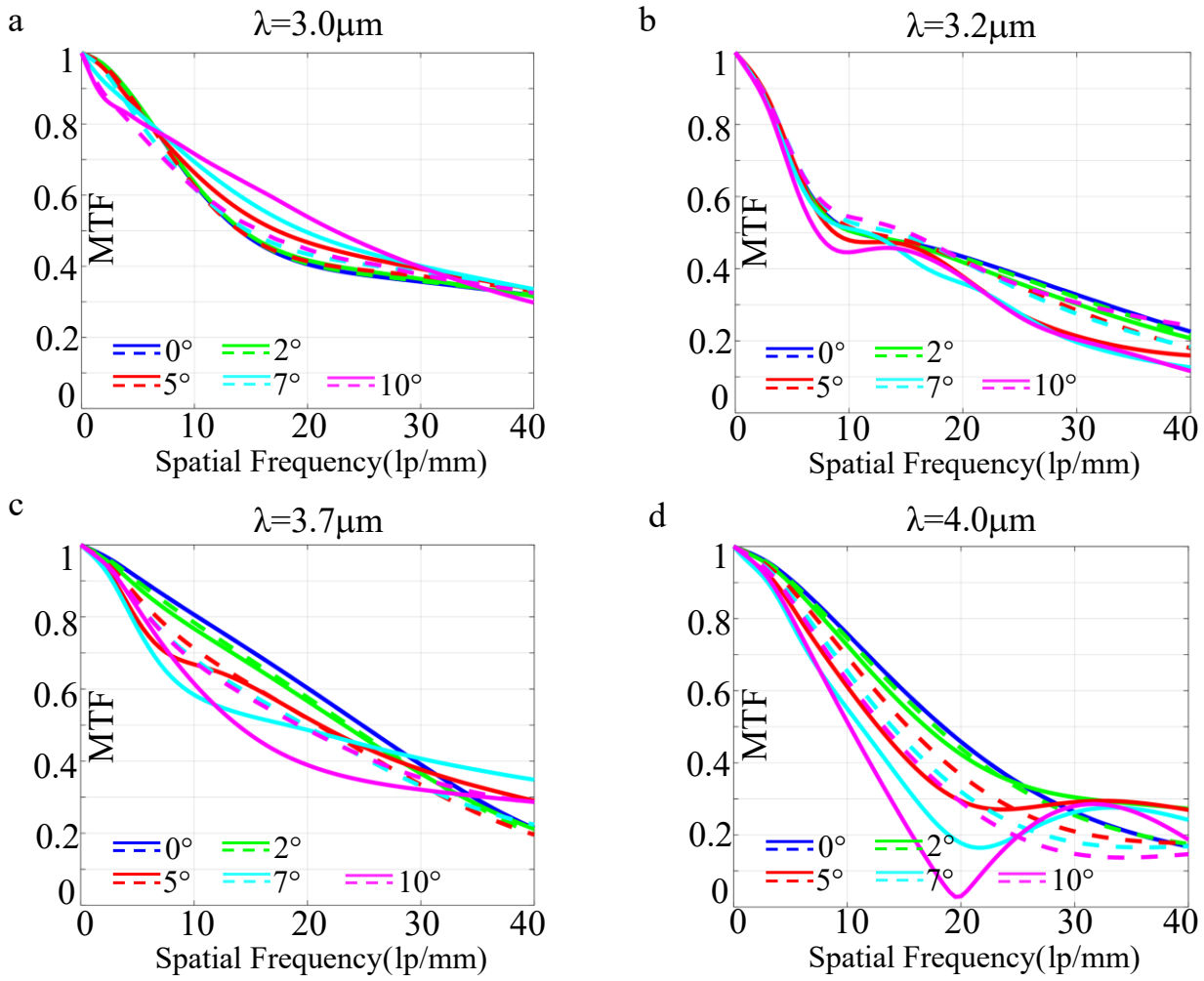

Fig. S1. The MTF analysis for the MWIR metalens with refractive lens and DOE at wavelengths of 3.0 μm, 3.2 μm, 3.7 μm, and 4.0 μm. (a) 3.0 μm, (b) 3.2 μm, (c) 3.7 μm, (d) 4.0 μm.

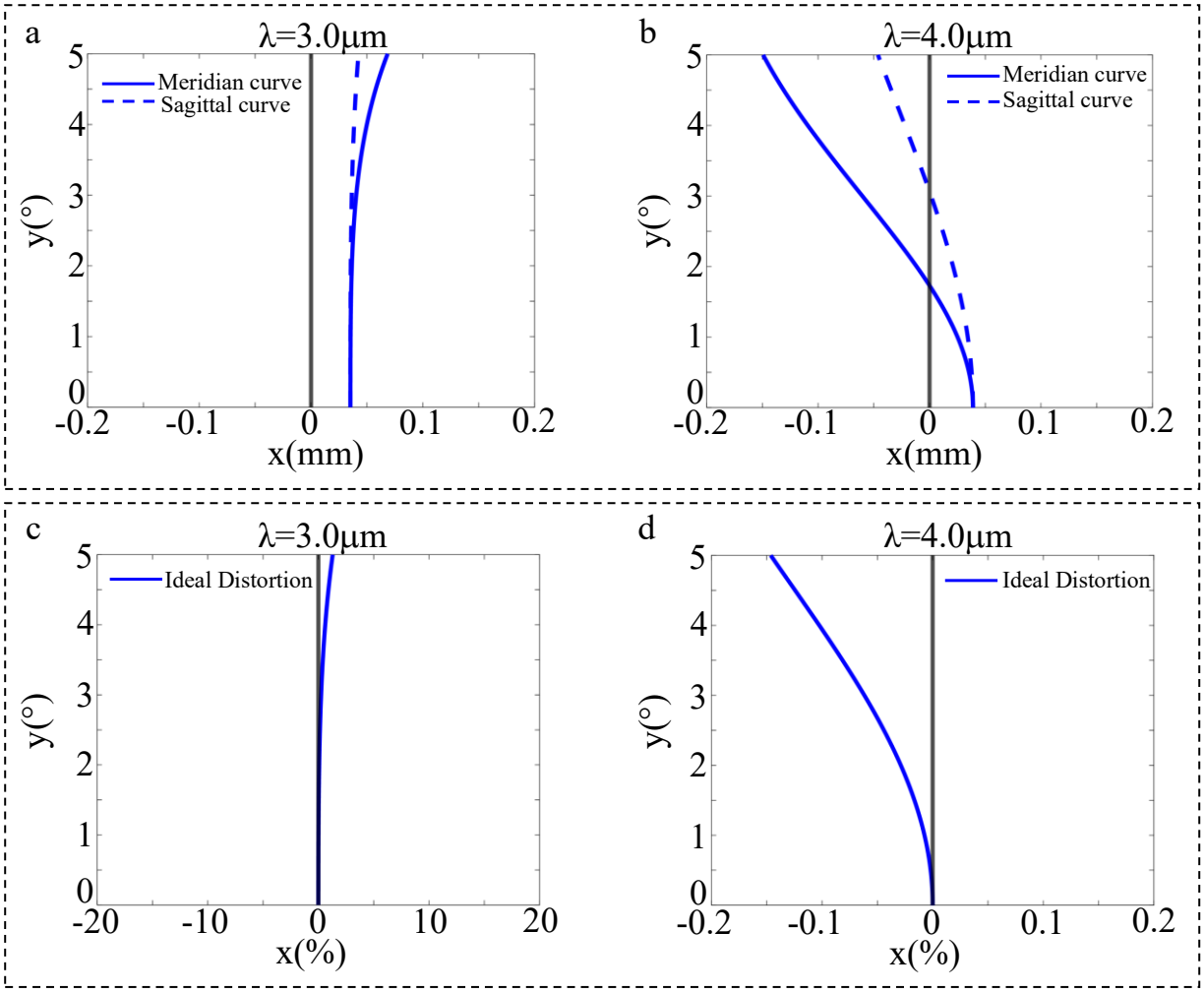

Fig. S2. (a-b) Field curvature assessments at wavelengths of 3.0 μm and 4.0 μm. (a) 3.0 μm, (b) 4.0 μm. (c-d) Distortion assessments at wavelengths of 3.0 μm and 4.0 μm. (c) 3.0 μm, (d) 4.0 μm.

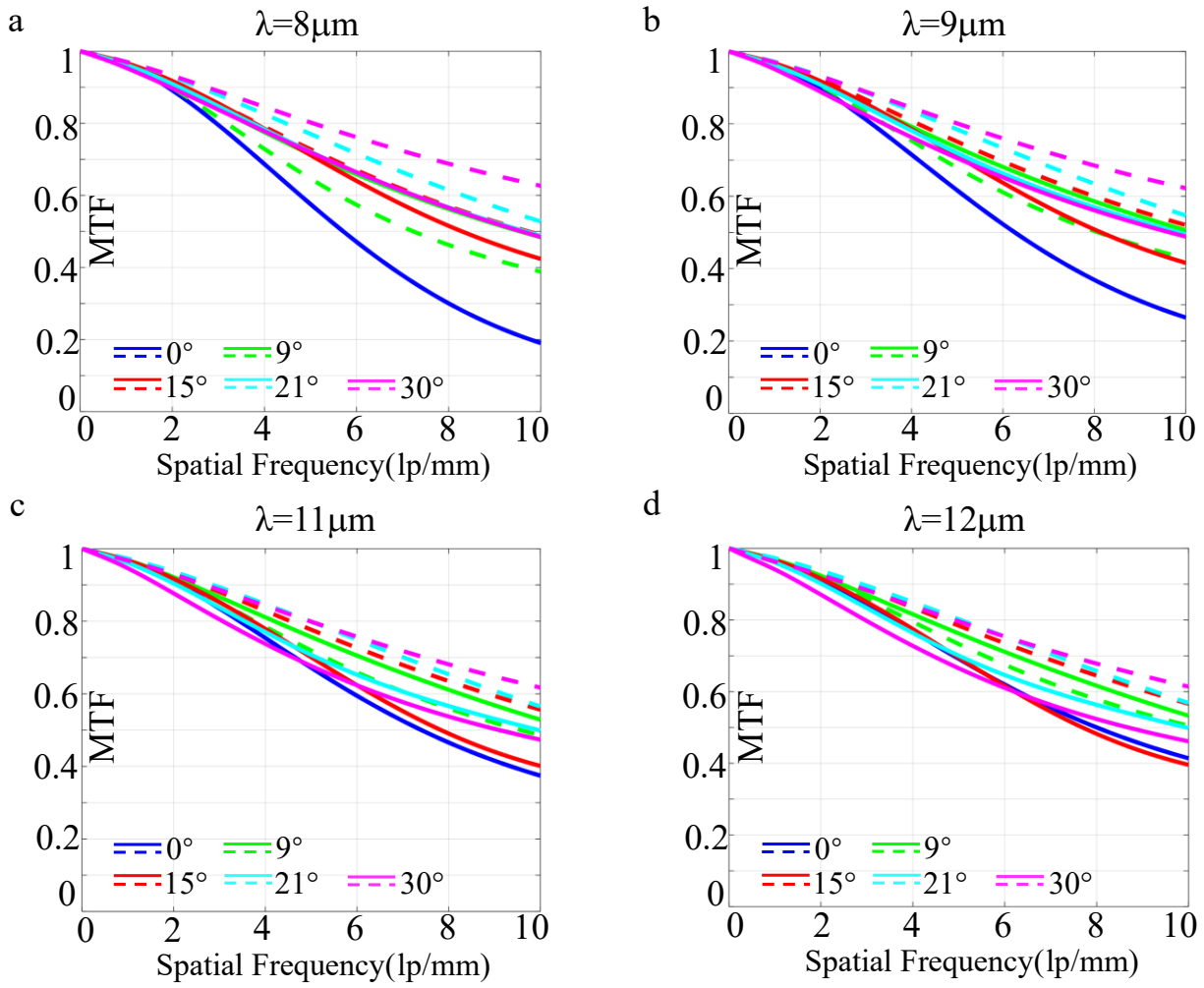

Fig. S3. The MTF analysis for the LWIR imaging with DOE at wavelengths of 8 μm, 9 μm, 10 μm, and 12μm. (a) 8 μm, (b) 9 μm, (c) 11 μm, (d) 12 μm.

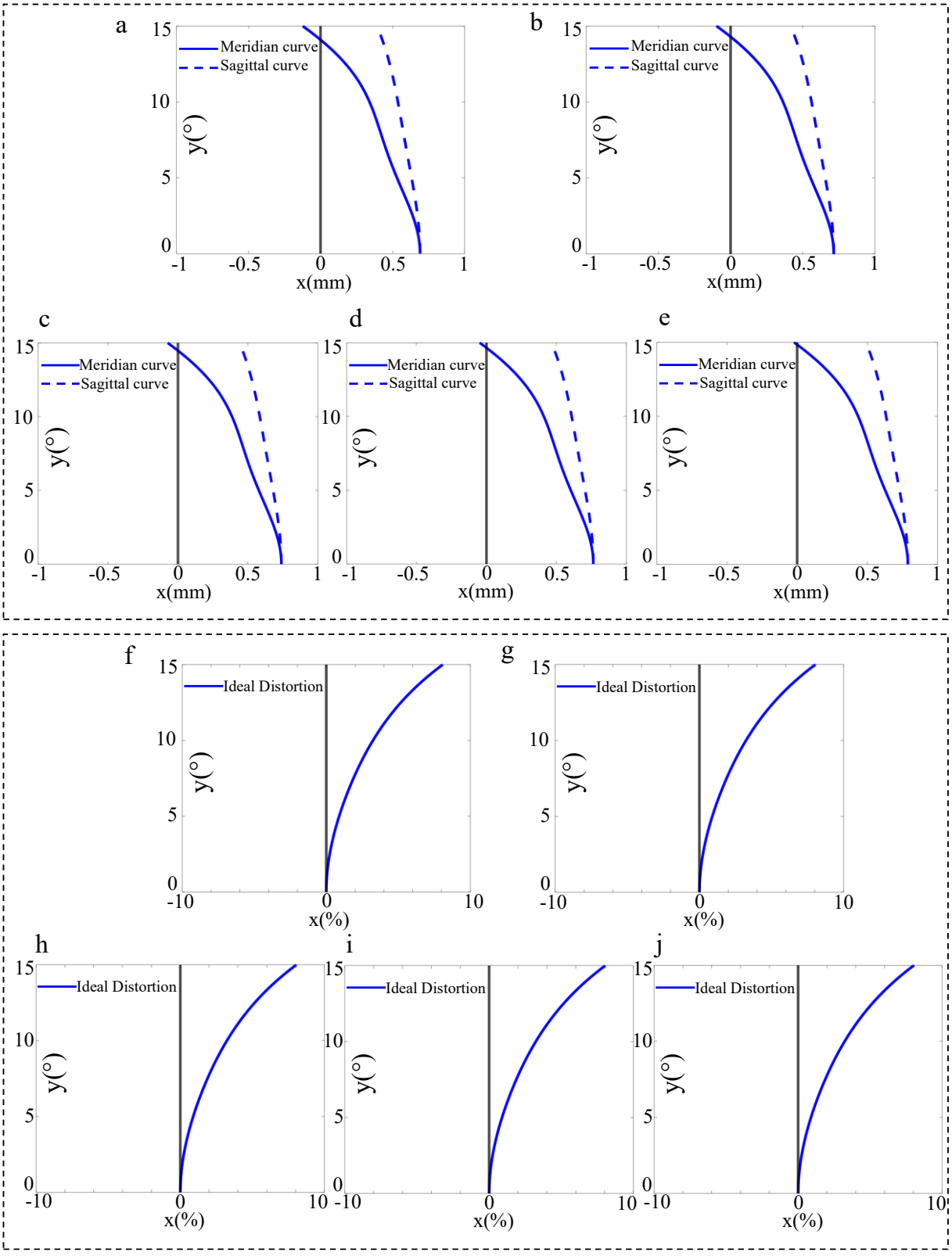

Fig. S4. (a-e) Field curvature assessments at wavelengths of 8 μm, 9 μm, 10 μm, 11 μm, and 12μm. (a) 8 μm, (b) 9 μm, (c) 10 μm, (d) 11 μm, (e) 12 μm. (f-j) Distortion assessments at wavelengths of 8 μm, 9 μm, 10 μm, 11 μm, and 12μm. (f) 8 μm, (g) 9 μm, (h) 10 μm, (i) 11 μm, (j) 12 μm.

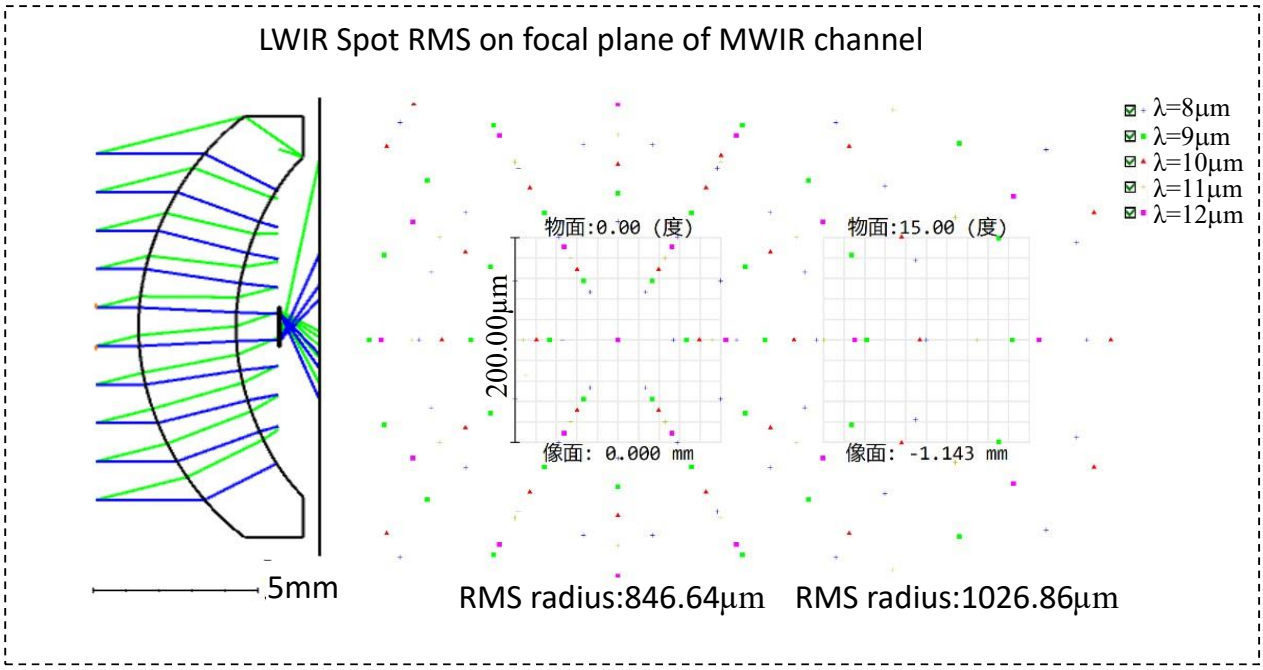

Fig. S5. RMS spot radius distribution in the MWIR channel under LWIR-band illumination at 0° and 30° FOV.

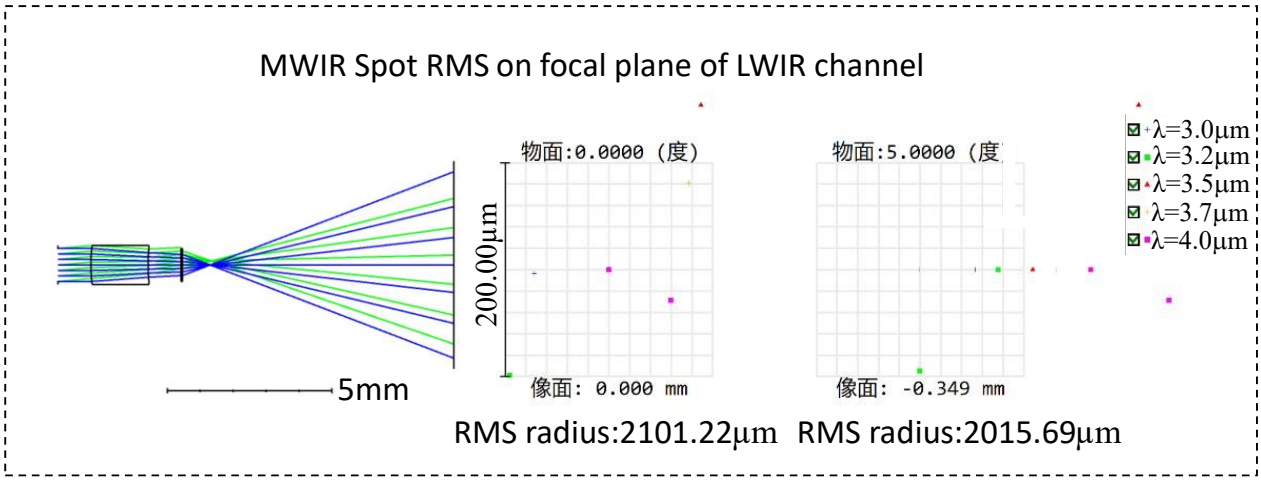

Fig. S6. RMS spot radius distribution in the LWIR channel under MWIR-band illumination at 0° and 10° FOV.

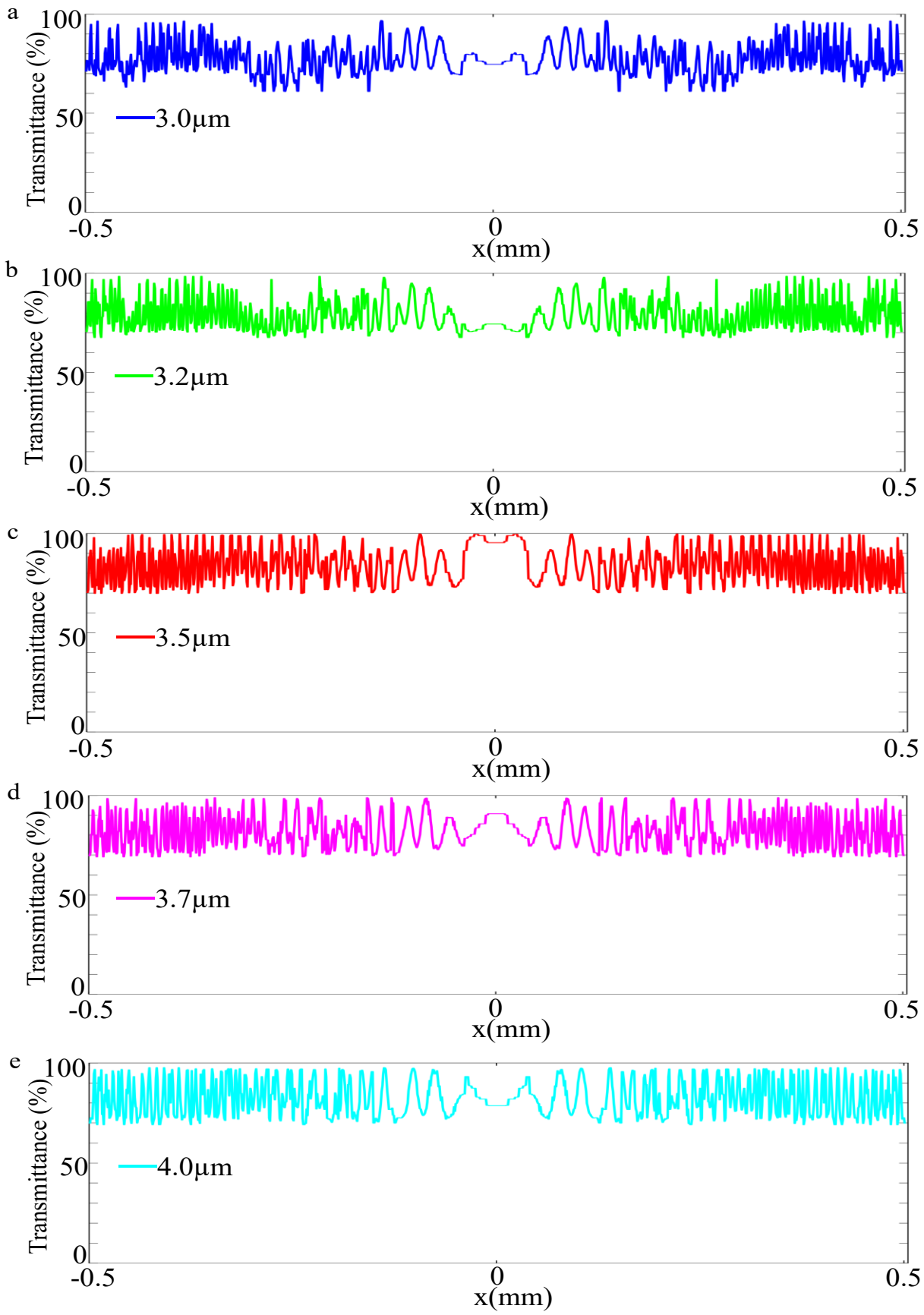

Fig. S7. The transmittance of the metalens at wavelengths of 3.0 μm, 3.2 μm, 3.5 μm, 3.7 μm, and 4.0μm. (a) 3.0 μm, (b) 3.2 μm, (c) 3.5 μm, (d) 3.7 μm, (e) 4.0 μm.

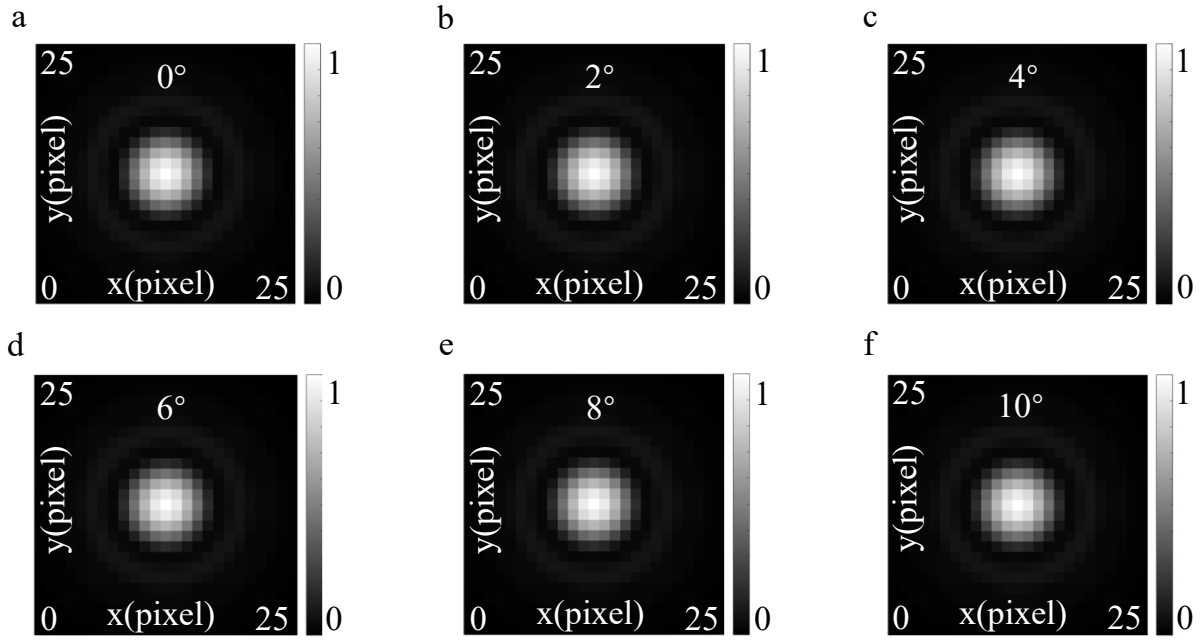

Fig. S8. Raw PSF intensity distributions on a 25 × 25 pixels grid, evaluated at six different FOV angles. (a) 0 degree, (b) 2 degree, (c) 4 degree, (d) 6 degree, (e) 8 degree, (f) 10 degree.

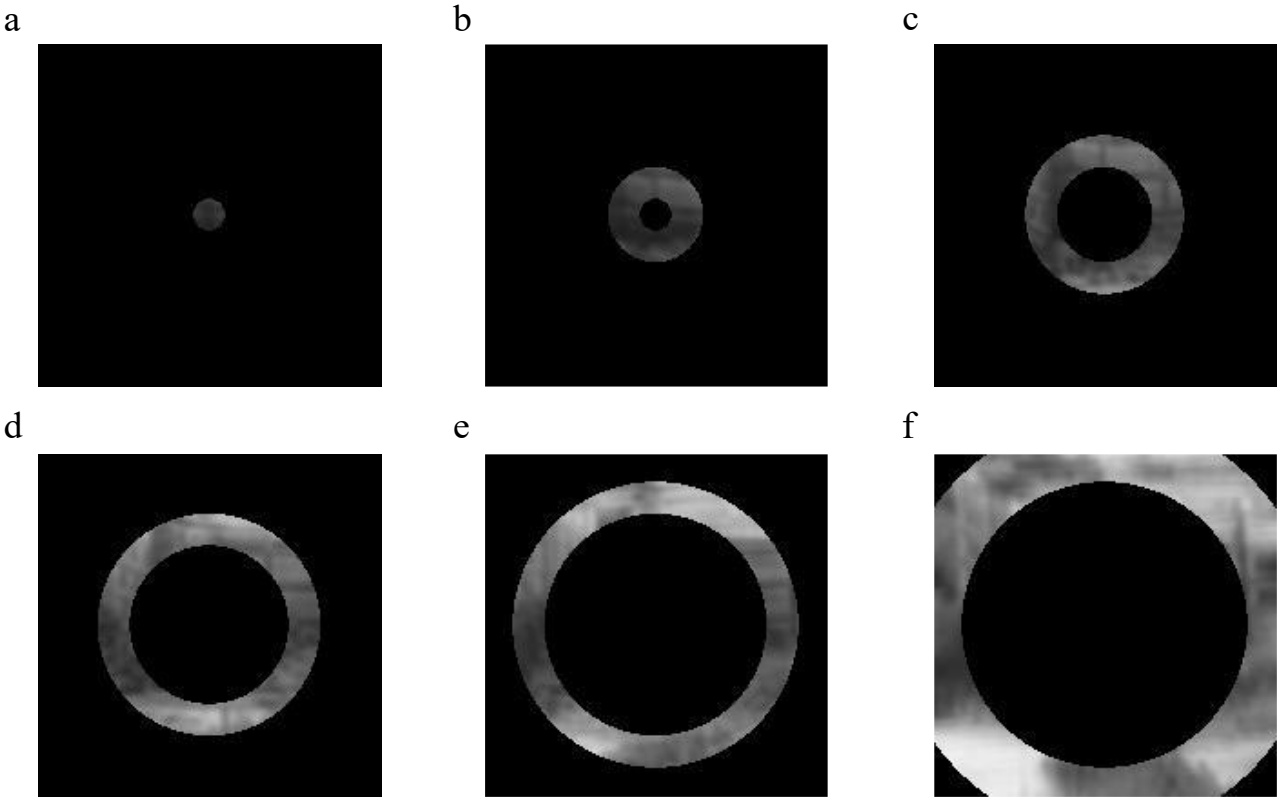

Fig. S9. The MWIR imaging results at six different FOV angles. (a) 0 degree, (b) 2 degree, (c) 4 degree, (d) 6 degree, (e) 8 degree, (f) 10 degree.

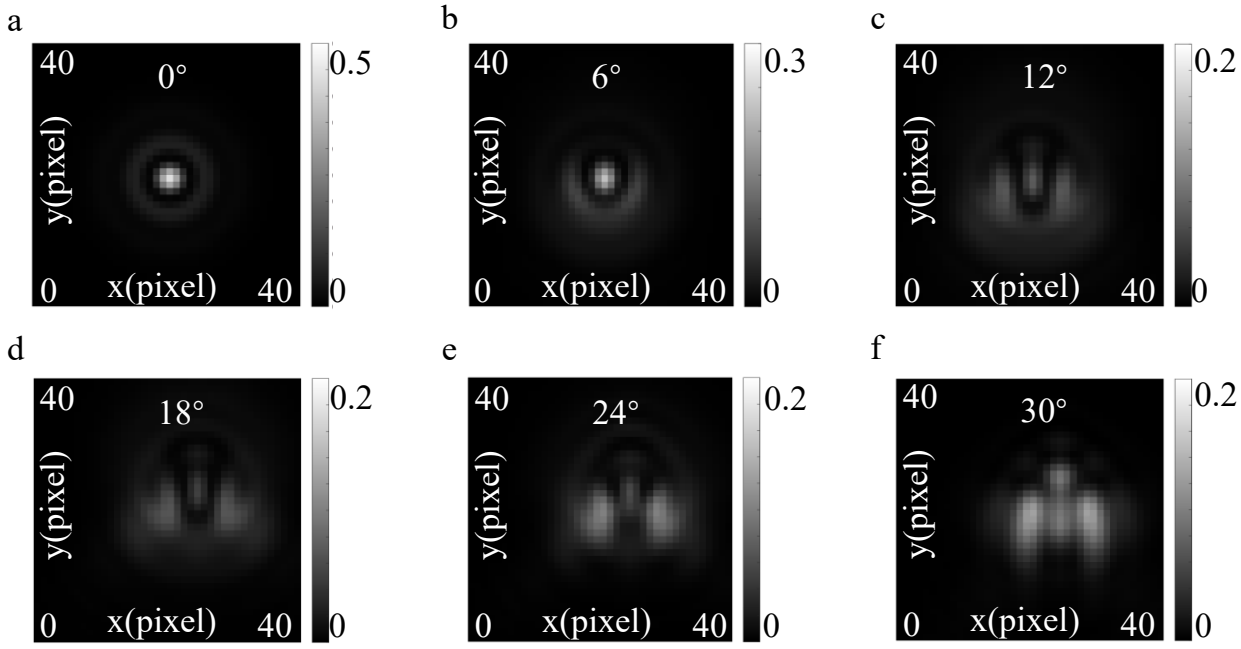

Fig. S10. Raw PSF intensity distributions on a 40 × 40 pixels grid, evaluated at six different FOV angles. (a) 0 degree, (b) 6 degree, (c) 12 degree, (d) 18 degree, (e) 24 degree, (f) 30 degree.

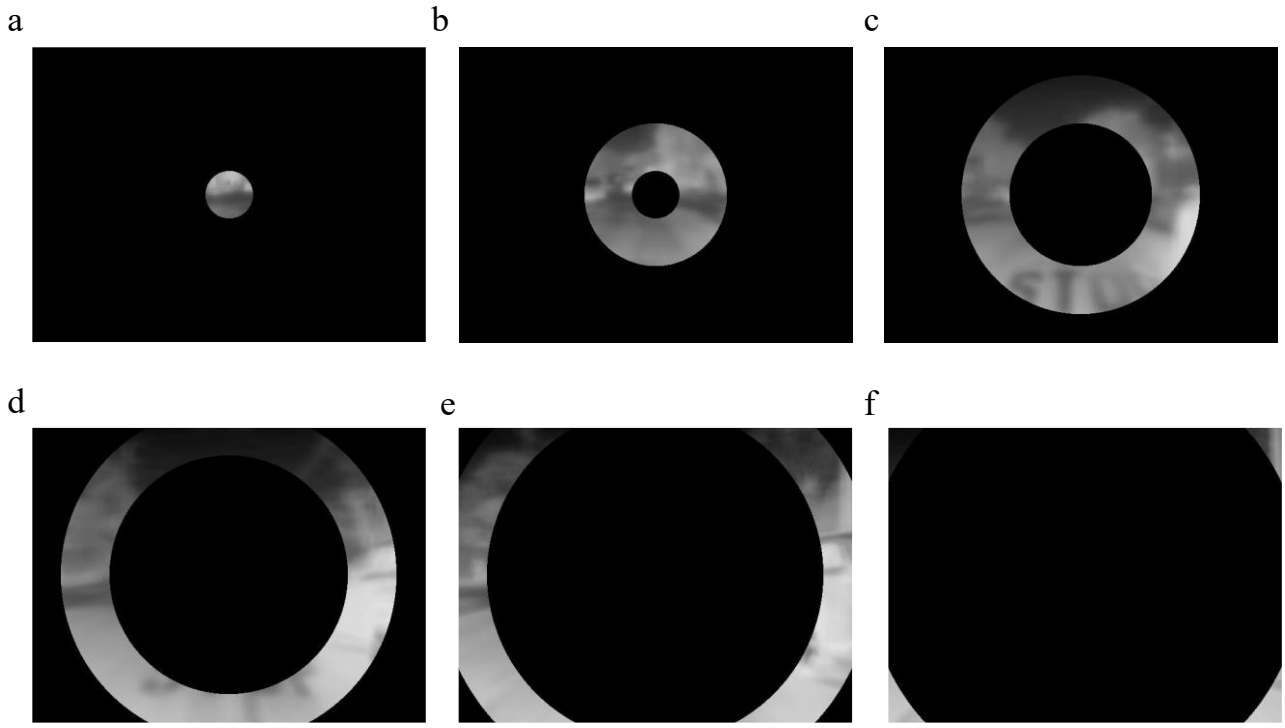

Fig. S11. The LWIR imaging results at six different FOV angles. (a) 0 degree, (b) 6 degree, (c) 12 degree, (d) 18 degree, (e) 24 degree, (f) 30 degree.

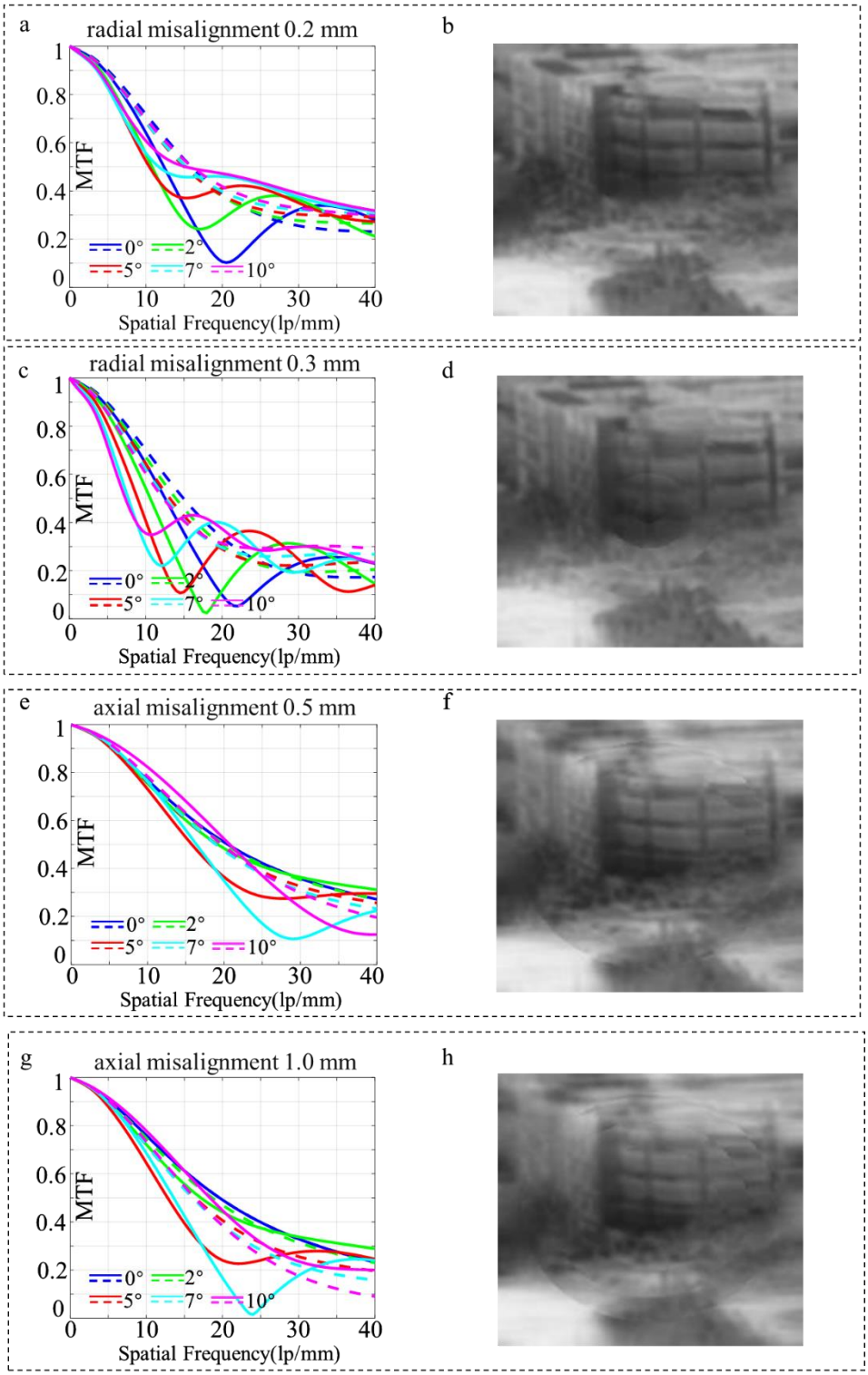

Fig. S12. MTF and imaging performance of the MWIR channel under misalignment between the metasurface and the refractive-diffractive element. (a-b) Radial (x-axis) misalignment of 0.2 mm: (a) MTF, (b) imaging result; (c-d) Radial misalignment of 0.3 mm: (c) MTF, (d) imaging result; (e-f) Axial (z-axis) misalignment of 0.5 mm: (e) MTF, (f) imaging result; (g-h) Axial misalignment of 1.0 mm: (g) MTF, (h) imaging result.

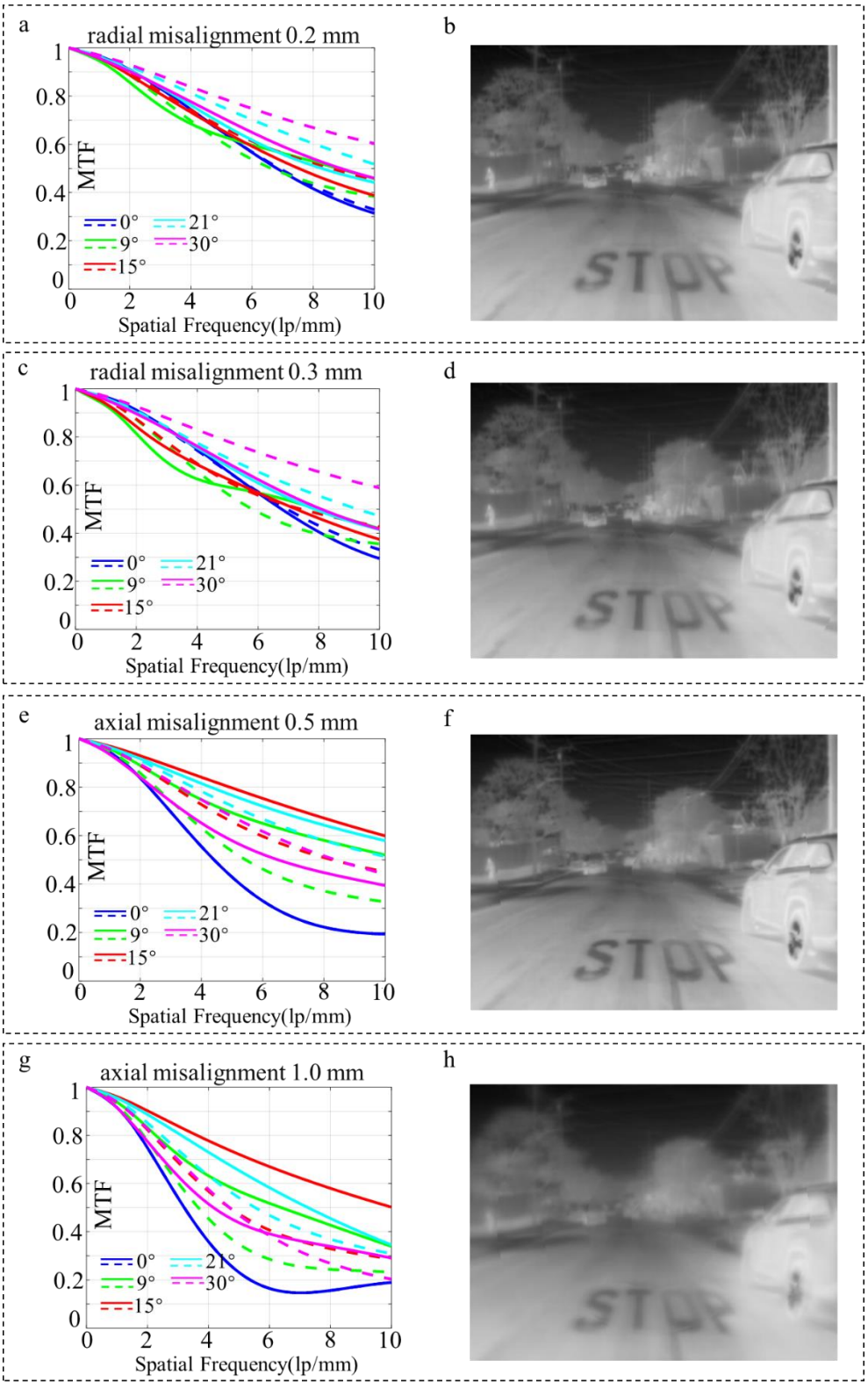

Fig. S13. MTF and imaging performance of the LWIR channel under misalignment between the metasurface and the refractive-diffractive element. (a-b) Radial (x-axis) misalignment of 0.2 mm: (a) MTF, (b) imaging result; (c-d) Radial misalignment of 0.3 mm: (c) MTF, (d) imaging result; (e-f) Axial (z-axis) misalignment of 0.5 mm: (e) MTF, (f) imaging result; (g–h) Axial misalignment of 1.0 mm: (g) MTF, (h) imaging result.

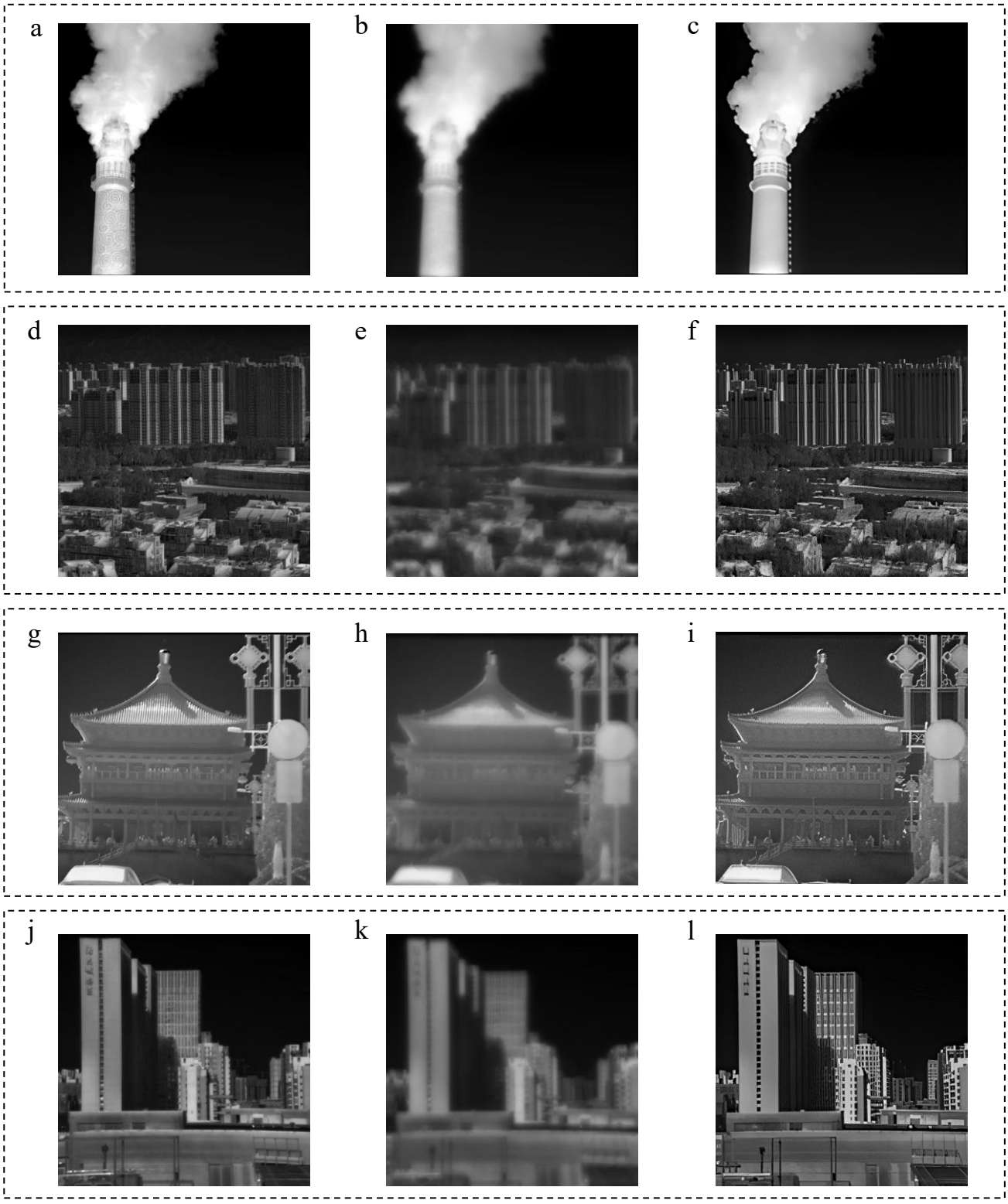

Fig. S14. MWIR imaging and image enhancement results across different scenes. The first column shows the ideal high-resolution MWIR test patterns, the second column presents the corresponding imaging results, and the third column displays the optimized images after enhancement.

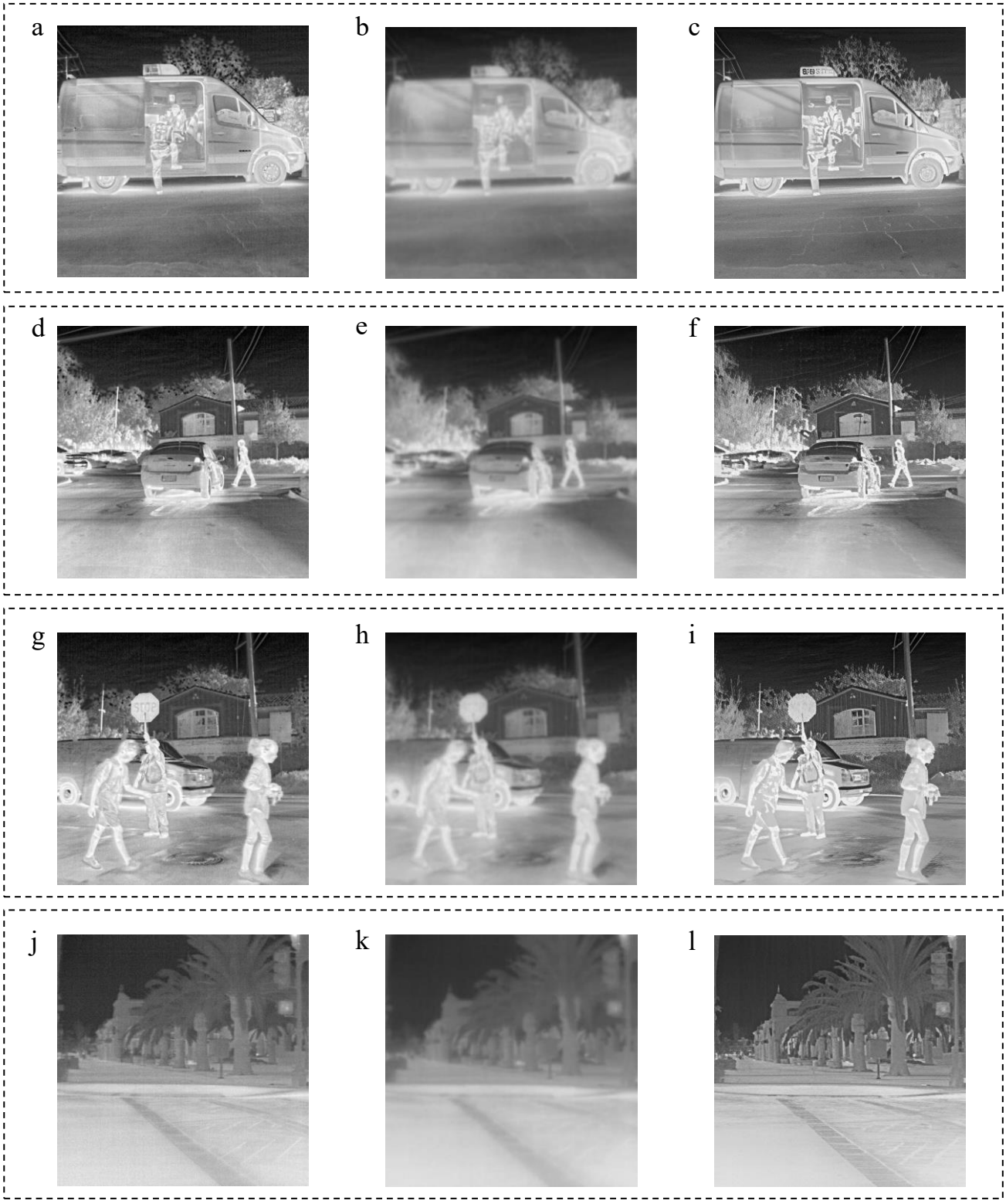

Fig. S15. LWIR imaging and image enhancement results across different scenes. The first column shows the ideal high-resolution LWIR test patterns, the second column presents the corresponding imaging results, and the third column displays the optimized images after enhancement.

Table S1. Comparison between the proposed system and existing MWIR-LWIR dual-band systems

Ref	Year	Bandwidth (μm)	MWIR FOV(º)	LWIR FOV(º)	N_RL (片)	N_DOE (片)	N_MS (片)	Image Enhancement
[9]	2015	4.4-5.4 &7.8-8.8	23	23	3	0	0	No
[12]	2019	3.0-5.0 & 8.0-11.0	30	30	4	0	0	No
[6]	2020	3.7-4.8 & 7.7-9.5	3	1.5	8	0	0	No
[10]	2020	3.7-4.8 & 7.7-9.3	33	33	10	0	0	No
[15]	2020	3.0-5.0 & 8.0-12.0	20	20	4	2	0	No
[14]	2022	3.7-4.8 & 8.0-12.0	8	8	3	2	0	No
[7]	2023	3.0-5.0 & 8.0-12.0	14	14	7	2	0	No
[11]	2025	3.7-4.8 & 7.7-9.5	66	66	8	0	0	No
[13]	2025	3.0-5.0 & 7.0-9.5	28-80	28-80	10	0	0	No
This work	2025	3.0-4.0 & 8.0-12.0	10	30	1	1	1	Yes